An Experimental Investigation of the Break-up of a Liquid Drop Falling in a Miscible Fluid

To cite this article: F. T. Arecchi *et al* 1989 *EPL* **9** 333

View the article online for updates and enhancements.

Related content

- Fragment Formation in the Break-up of a Drop Falling in a Miscible Liquid
  F. T. Arecchi, P. K. Buah-Bassuah and C. Perez-Garcia

- 2D Dynamics of a Drop Falling in a Miscible Fluid
  A. Garcimartín, H. L. Mancini and C. Pérez-García

- Phenomena of liquid drop impact on solid and liquid surfaces
  Martin Rein

Recent citations

- Gravitational instabilities in binary granular materials
  Christopher P. McLaren *et al*

- Colloid Transport in Porous Media: A Review of Classical Mechanisms and Emerging Topics
  Ian L. Molnar *et al*

- Mode selection on breakup of a droplet falling into a miscible solution
  Michiko Shimokawa and Hidetusgu Sakaguchi

An Experimental Investigation of the Break-up of a Liquid Drop Falling in a Miscible Fluid.

F. T. ARECCHI(*), P. K. BUAH-BASSUAH(**), F. FRANCINI
C. PÉREZ-GARCIA(***) and F. QUERCIOLI
Istituto Nazionale di Ottica, Largo Enrico Fermi 6 - 50125 Arcetri (Firenze), Italy

Abstract. – A liquid drop falling in a lighter miscible fluid either undergoes a cascade of fragmentations, each appearing as a dynamic instability, or it mixes by diffusion, depending on the value of a fragmentation number F. F is the ratio of the diffusion time to the time required for the fluid to convectively mix. We assign an accurate experimental value to the critical fragmentation number F_c, which appears to be universal. When the fragmentation occurs, the interfacial area increases via successive splittings which display striking symmetries. We present experimental evidence and a qualitative explanation of such a phenomenon.

Hydrodynamic instabilities provide many case studies of spatio-temporal organization in extended macroscopic systems [1]. We must distinguish between instabilities in confined systems and in open flows. In the former case, spatial effects are affected by boundaries, as for example in the Rayleigh-Benard (RB) [2] and Taylor-Couette (TC) flows [3, 4]. Likewise, in open flows many pattern forming effects have been classified, such as the von Kármán instability at the boundary layer of a flow passing round a cylinder, the Kelvin-Helmholtz (KH) instability at the interface between two fluids moving with different velocities and the Rayleigh-Taylor (RT) instability when a heavier fluid stands above a lighter one [1, 3, 5, 6].

The purpose of this letter is to report on the evolution of a liquid drop falling through a lighter miscible liquid confined in a vessel much larger than the drop size. The result is an open hydrodynamic instability described by Helmholtz [7] and Thomson *et al.* [8] in the last century and which can be viewed as one of the simplest in an open system. It has some of the characteristics of the KH and RT instabilities, and it is by far easier to observe experimentally, even though, at present, no theory exists to explain it.

(*)   Also with the Dipartimento di Fisica, Università di Firenze, Firenze, Italy.
(**)   Permanent address: Department of Physics, University of Cape Coast, Cape Coast, Ghana.
(***) On leave from Departament de Fisica, Universitat Autonoma de Barcelona, 08193 Bellaterra (Barcelona), Catalonia, Spain.

We fill a long transparent vessel with a liquid and carefully release onto the free surface a drop of the heavier liquid with zero initial velocity. The drop volume is controlled by a micro-syringe. All reported experiments have been performed under isothermal conditions at a temperature of 20 °C. Initially the drop behaves as a falling body where the downward force due to gravity is proportional to the density difference $\Delta\varrho$ of the two fluids. After a transient ruled by a time constant $\tau' \simeq \varrho r^2/\mu$ (ϱ = drop density, r = drop radius, μ = viscosity of the surrounding fluid); (here and below, we skip multiplicative constants of order unity), the drop motion reaches steady state whereby the gravity force is compensated by the Stokes force, which in turn is proportional to the product of the drop velocity and the viscosity μ. In all our experiments the equilibration time τ' is at most 0.1 s, that is neglegible with respect to the time scales of the main phenomena. Furthermore, the Reynolds number R is always of the order of unity, even for the largest drop, thus Stokes approximation can still be used to build a qualitative argument [9]. Hence, in the sedimentation regime, the asymptotic velocity v_∞ scales as $v_\infty \simeq g \Delta\varrho r^2/\mu$.

For a convenient observation of the initial stages, the evolution of the drop can be slowed down by playing on the quantity $\Delta\varrho/\mu$. Using a solution of glycerin and water in the volume ratio 60 : 40 in the vessel and heavier drops of glycerin-water in volume ratios from 70 : 30 to 90 : 10, the sequence of phenomena is qualitatively the same for drops of radii r within a range specified later.

We experimentally observed the evolution of the falling drop in two ways: 1) laterally, where pictures were recorded from a translucent paper glued to the opposite side of the cell and facing the incoming white light, and 2) vertically, where the image of the drop was projected on the bottom when we shine from the top with an expanded laser beam. The image contrast relies on the lensing effects provided by small differences in the refractive index between the two fluids. Data are recorded by a standard CCD camera on a TV tape.
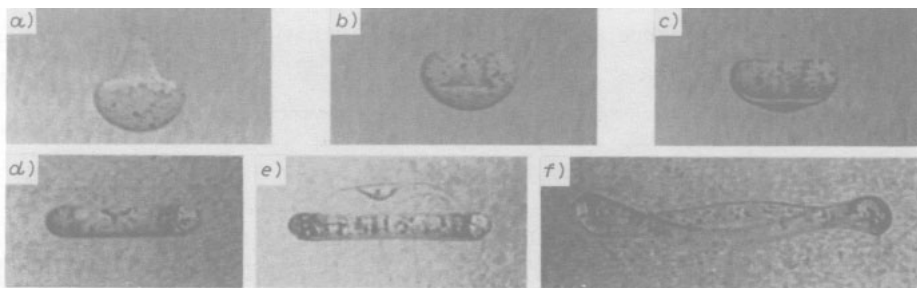

Fig. 1. – Evolution of a falling liquid drop with $r = 0.29$ cm and $\Delta\varrho = 0.0789$ g/cc. $a)$-$f)$ Sequence of lateral views of the drop motion taken at the following positions from the free surface and times from the deposition: $a)$ 2.0 cm, 1.05 s; $b)$ 6.0 cm, 3.03 s; $c)$ 8.0 cm, 4.0 s; $d)$ 10.0 cm, 5.2 s; $e)$ 13.0 cm, 7.34 s; and $f)$ 16.0 cm, 10.0 s. $e)$ shows the appearance of the turban instability, and $f)$ the torus breaking by RT instability.

In fig. 1 we show the phenomenology through a sequence of successive frames. The drops, composed of 90% glycerin and 10% water, and with initial radius $r \simeq 1$ mm, have been seeded with tiny carbon particles (of size around 70 μm) for the sake of demonstration of the vortex motions. However, most of the experimental observations (successive figures) refer to nonseeded drops with a concentration 70 : 30.

A qualitative interpretation of the results is the following. In the initial stages, the falling drop tends to generate a region with growing vorticity as a consequence of shear at the interface between the two fluids. Thus in the centre-of-mass system of the falling drop, the

drop edges move upwards. This mechanism, similar to that responsible for KH instability, tends to deform the drop into the shape of a mushroom (fig. 1b)). Combination of the vertical velocity with the angular velocity transferred by shear induces a radial drift, hence the mushroom expands horizontally. This resembles the vortex ring formation at a nozzle [9]. Indeed, the mushroom shape assumed by a falling drop suggested the identification with a vortex ring to Thomson [8]. However, a very essential phenomenon was overlooked in those observations.

In the further evolution of the mushroom, there exists a membrane which connects continuously the drop's bottom part. From fig. 1a)-c), this membrane is convex as viewed from below, but it gets thinner during the radial expansion. Eventually the membrane's curvature changes sign from convex to concave as observed in fig. 1d) and e). Once the concavity is formed, the ring is exposed to shear both in its inner and outer parts and hence the circulation is rapidly slowed down to a full stop. We consider the change of sign in the curvature of the bottom membrane as the onset of what we call *turban instability* (just after fig. 1d)) since the deformed drop looks like a *turban*. This instability builds up rapidly since, as matter flows by gravity from the trailing membrane to the ring, the membrane's sedimentation velocity reduces further with respect to that of the ring. The above qualitative description is supported by a quantitative appreciation of the decay of the circulation in the slowing-down of the tracing particles in successive frames. Such a behaviour is at variance with that of a standard vortex ring, where, apart from the relatively small losses due to viscosity, the circulation is conserved (Kelvin's theorem) [10].

After the onset of the turban instability, the radial expansion of the ring tends to stop and eventually the torus becomes unstable by the RT instability. Indeed the fluid inside the torus is heavier than the liquid below, hence a small perturbation in the height of the torus results in a destabilizing pressure change which breaks the torus at two or more points, depending on the drop size (fig. 1f)). The liquid inside the ring falls towards these points, thus the whole *turban* (ring plus membrane) looses its round symmetry, stretching along a line joining the instability points. (This is better appreciated from the top views, fig. 3b) and c), to be discussed later.) The regions around the instability points are filled by the falling matter, and they generate secondary drops which undergo exactly the same process but oriented at right angles to the primary drop. Henceforth, by combination of turban and RT instability, each secondary drop will produce tertiary drops and so on, as shown in fig. 2.
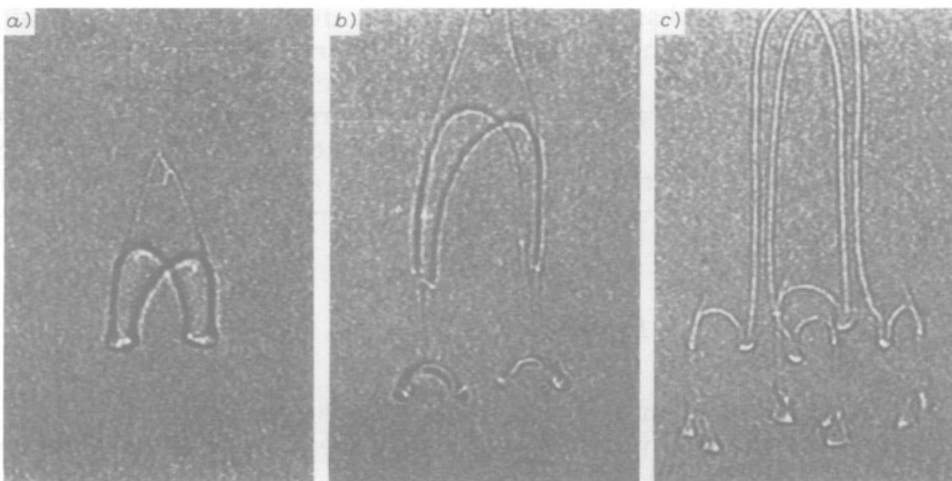

Fig. 2. – Lateral views of the fragmentation process for experiment 9 of table I. Space-time data, defined as in fig. 1, are: a) 13.0 cm, 27.52 s; b) 17.0 cm, 44.86 s; c) 24.0 cm, 93.08 s.

The successive divisions lead to a cascade of multiple pairs of secondary droplets forming a finely divided ensemble (fig. 2c)).

These observations are confirmed by taking the shadowgraph of the drop shined vertically. In fig. 3, a typical sequence is shown. A regular torus is evident in fig. 3a), and after being destabilized it stretches into an elliptical shape (fig. 3b)). Secondary droplets are formed at the extremes of the major axis, and then expand normally to that axis (fig. 3c). Each secondary droplet gives rise to two tertiary droplets (fig. 3d)).
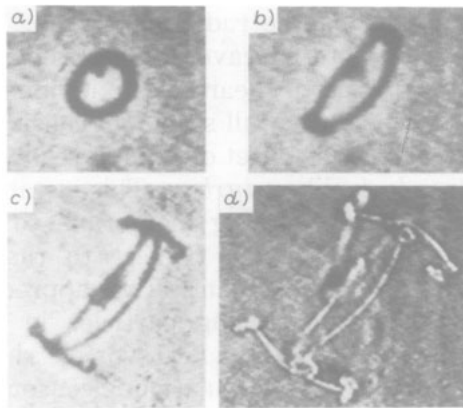

Fig. 3. – Vertical projection of the falling drop (bottom view). Sequence of four frames (a)-d)) of space-time evolution. The measured times of the frames are a) 10, b) 25, c) 35, d) 85 s.

This cascade of fragmentations eventually stops for the following reasons. Diffusion becomes more and more effective for small radii, because its characteristic time reduces as $\tau \simeq r^2/D$, where D is the diffusion coefficient between the two fluids. As the sedimentation velocity decreases, by reduction of both $\Delta\varrho$ and r, the circulation transferred by shear and responsible for ring formation reduces also, until a situation is reached where the diffusion time is shorter than the onset time of the turban instability. From here on the drops disappear by pure diffusion without further shape transformation. In the experiment of fig. 2 and 3, this occurs after three divisions.

The borderline between turban instability and drop disappearance by diffusion can be assigned via an adimensional number F expressed as the ratio of two characteristics times. Fragmentation of a drop falling with the asymptotic velocity v_∞ implies the onset of a circular velocity, and this requires at least a time τ_1 corresponding to the transfer of v_∞ across the drop radius, that is, $\tau_1 = r/v_\infty \simeq \mu/(\Delta\varrho g r)$. Such a process is counteracted by diffusion, which takes place over the time τ. As expected, and observed experimentally, the fragmentation stops at a radius where τ_1 becomes longer than fixed fraction of τ, that is fragmentation occurs when

$$F = \frac{\tau}{\tau_1} = \left(g\, \frac{\Delta\varrho}{\mu}\, \frac{V}{D} \right) > F_c. \tag{1}$$

Here F is the fragmentation number and F_c has to be specified empirically. We have expressed F in terms of the drop volume V rather than the cubic power of its radius, since V is a directly measurable quantity.

As we seed drops with $F > F_c$, fragmentation stops when the daughter drop volume is such that $F \leq F_c$, while, if the initial drop has $F < F_c$ no fragmentation occurs. An accurate

calibration of F_c has been performed over eight samples, which differ either in glycerin-water ratios of solvent, or drop or in drop volume. The data are reported in table I and fig. 4.

TABLE I.

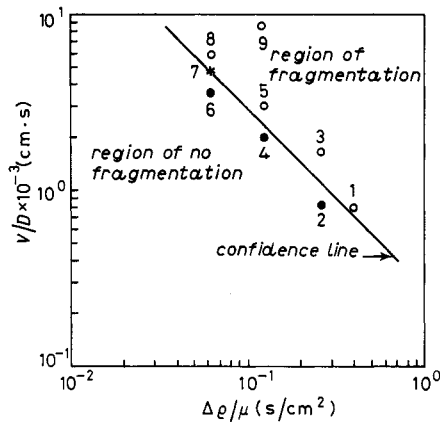| Exp no.	Volume ratio glycerin/water		μ $g \cdot cm^{-1} \cdot s^{-1}$	$\Delta\rho \cdot 10^2$ $(g \cdot cm^{-3})$	$V \cdot 10^3$ (cm^3)	$D \cdot 10^6$ $(cm^2 \cdot s^{-1})$	Results	
	Solvent	Drop					ε	Fragmentation
1	60/40	75/25	0.11	3.9	1.0	1.25	0.11	Y
2	60/40	70/30	0.11	2.6	1.0	1.20	-0.23	N
3	60/40	70/30	0.11	2.6	2.0	1.20	0.52	Y
4	70/30	80/20	0.21	2.6	2.0	0.98	-0.12	N
5	70/30	80/20	0.21	2.6	3.0	0.98	0.24	Y
6	70/30	75/25	0.21	1.3	3.0	0.84	-0.25	N
7	70/30	75/25	0.21	1.3	4.0	0.84	0.00	Y/N
8	70/30	75/25	0.21	1.3	5.0	0.84	0.21	Y
9	60/40	70/30	0.11	2.6	10.5	1.20	2.63	Y

Fig. 4. – Plot of V/D vs. $\Delta\rho/\mu$ (log-log scale) close to the onset of fragmentation for nine experimental situations numbered as in table I. Each measured point is repeated several times. The confidence line corresponds to $F_c = g(\Delta\rho \cdot V/\mu \cdot D)_c = (2.8 \pm 0.1) \cdot 10^5$. Experiment 9 ($\varepsilon = 2.63$) yields three fragmentations before diffusing away. It corresponds to the sequence reported in fig. 2, 3.

The viscosity data are interpolated from the tables of ref. [11] and drop volumes have been accurately calibrated by a micro-syringe. As for diffusion no accurate data were available in the literature, thus the values of D reported in table I were measured by using a laser light deflection method [12] (details will be reported elsewhere). The points 1-8 reported in table I and fig. 4 represent the closest approach achievable to the demarcation line between pure diffusion (N = no fragmentation, Y = fragmentation and Y/N = fragmentation in 50% of cases). The line drawn is a suitable confidence line; it corresponds to a value $F_c =$ $= (2.8 \pm 0.1) \cdot 10^5$. For each point of table I, we report the relative fragmentation number $\varepsilon = F/F_c - 1$. $\varepsilon = 0$ marks the onset of the turban instability. As we increase ε above zero, the number of successive fragmentations increases. In order to reach three fragmentations as shown in fig. 2 and 3, we had to go to $\varepsilon = 2.63$ (point 9 of table I and fig. 4).

These phenomena have been tested on other fluids (water and salty water, or different alcoholic mixtures). Regimes at high ε yield a number of fragmentations much larger than three. In such cases, we can describe the instantaneous shapes in terms of a spectrum of scale lengths. The dependence of this spectrum on ε will be reported elsewhere.

Experiments have also been performed with drops of lighter fluid introduced at the bottom of the vessel through a capillary tube. We observed similar cascades reversed along the vertical direction. As seen from the different size and composition of the samples, F_c is a universal number, independent of the nature of the two miscible liquids. We have thus assigned a reliable demarcation line between diffusion and fragmentation phenomena.

* * *

REFERENCES

[1] *Propagation in Systems far from Equilibrium*, edited by J. E. WESFREID *et al.* (Springer-Verlag, Berlin) 1988.
[2] CILIBERTO S. and BIGAZZI P., *Phys. Rev. Lett.*, **60**(4) (1988) 286; KOLODNER P., BENSIMON D. and SURKO C. M., *Phys. Rev. Lett.*, **60**(17) (1988) 1723.
[3] See the *Proceedings of the* IUTAM *Symposium Fluid Mechanics in the Spirit* of TAYLOR G. I., *J. Fluid Mech.*, **173** (1986) and the special volume *Front Interfaces and Patterns*, in *Physica D*, **12** (1984).
[4] DOMÍNGUEZ-LERMA M. A., CANNELL D. S. and AHLERS G., *Phys. Rev. A*, **34** (1986) 4956.
[5] CHANDRASEKHAR S., *Hydrodynamic and Hydromagnetic Stability* (Dover, New York, N.Y.) 1981.
[6] TRITTON D. J., *Physical Fluid Dynamics*, 2nd edition (Clarendon Press, Oxford) 1988.
[7] HELMHOLTZ H., *Berl. Mber.* (1868) 215 (also *Philos. Mag.*, **36**(4) (1868) 337).
[8] THOMSON J. J. and NEWALL H. F., *Proc. R. Soc. London*, **39** (1885) 417.
[9] BATCHELOR G. K., *An introduction to fluid dynamics* (Cambridge University Press, Cambridge) 1967.
[10] Sir WILLIAM THOMSON (Lord Kelvin), *Philos. Mag.*, **10**(5) (1880) 97.
[11] LANDOLT-BÖRNSTEIN, *Numerical data and functional relationships*, new series, edited by K. H. HELLWEGE, Vol. 5, Band 2 (Springer-Verlag, Berlin) 1979.
[12] GIGLIO M. and VENDRAMINI A., *Phys. Rev. Lett.*, **34**(10) (1975) 561.